Cell Reports

Report

Energy Stress Regulates Hippo-YAP Signaling Involving AMPK-Mediated Regulation of Angiomotin-like 1 Protein

Graphical Abstract

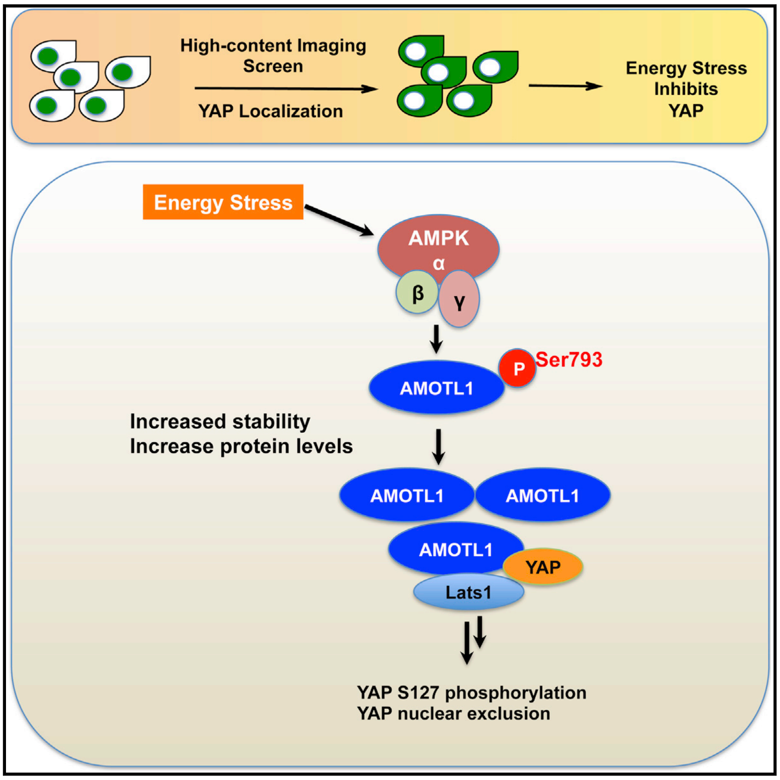

Highlights

Energy stress inhibits YAP

AMPK is required to mediate the effects

AMPK directly phosphorylates AMOTL1, an upstream inhibitor of YAP, at S793

AMOTL1 S793 phosphorylation affects its stability

Authors

Michael DeRan, Jiayi Yang, ..., Jun Liu, Xu Wu

Correspondence

xwu@cbrc2.mgh.harvard.edu

In Brief

DeRan et al. discovered that cellular energy level is an upstream regulator of Hippo-YAP pathway. Energy stress, such as inhibition of glucose metabolism and ATP production, could inhibit YAP activity. This process requires the central metabolic sensor AMPK, which directly phosphorylates and stabilizes AMOTL1, an upstream regulator of YAP.

CrossMark

DeRan et al., 2014, Cell Reports 9, 495–503
October 23, 2014
http://dx.doi.org/10.1016/j.celrep.2014.09.036

CellPress

Cell Reports
Report

Energy Stress Regulates Hippo-YAP Signaling Involving AMPK-Mediated Regulation of Angiomotin-like 1 Protein

Michael DeRan,[1,5] Jiayi Yang,[2,5] Che-Hung Shen,[1] Eric C. Peters,[2] Julien Fitamant,[3] Puiyee Chan,[1] Mindy Hsieh,[2] Shunying Zhu,[1] John M. Asara,[4] Bin Zheng,[1] Nabeel Bardeesy,[3] Jun Liu,[2] and Xu Wu[1,*]
[1]Cutaneous Biology Research Center, Massachusetts General Hospital, Harvard Medical School, Charlestown, MA 02129, USA
[2]Genomics Institute of the Novartis Research Foundation, San Diego, CA 92121, USA
[3]Massachusetts General Hospital Cancer Center, Harvard Medical School, Boston, MA 02114, USA
[4]Division of Signal Transduction, Beth Israel Deaconess Medical Center, Harvard Medical School, Boston, MA 02115, USA
[5]Co-first author
*Correspondence: xwu@cbrc2.mgh.harvard.edu
http://dx.doi.org/10.1016/j.celrep.2014.09.036

SUMMARY

Hippo signaling is a tumor-suppressor pathway involved in organ size control and tumorigenesis through the inhibition of YAP and TAZ. Here, we show that energy stress induces YAP cytoplasmic retention and S127 phosphorylation and inhibits YAP transcriptional activity and YAP-dependent transformation. These effects require the central metabolic sensor AMP-activated protein kinase (AMPK) and the upstream Hippo pathway components Lats1/Lats2 and angiomotin-like 1 (AMOTL1). Furthermore, we show that AMPK directly phosphorylates S793 of AMOTL1. AMPK activation stabilizes and increases AMOTL1 steady-state protein levels, contributing to YAP inhibition. The phosphorylation-deficient S793Ala mutant of AMOTL1 showed a shorter half-life and conferred resistance to energy-stress-induced YAP inhibition. Our findings link energy sensing to the Hippo-YAP pathway and suggest that YAP may integrate spatial (contact inhibition), mechanical, and metabolic signals to control cellular proliferation and survival.

INTRODUCTION

Hippo signaling has been implicated in organ size control by restricting the transcriptional coactivators YAP/TAZ (Dong et al., 2007; Harvey and Tapon, 2007; Harvey et al., 2013; Pan, 2007). The core components of the pathway construct a kinase cascade, in which Mst1/Mst2 in complex with SAV1 phosphorylate and activate Lats1/Lats2 kinases. Subsequently, Lats1/Lats2 kinases in complex with Mob1 phosphorylate YAP/TAZ, leading to their cytoplasmic retention and inhibition (Harvey et al., 2003; Udan et al., 2003; Wu et al., 2003). Inhibition of this kinase cascade leads to dephosphorylation of YAP/TAZ and their accumulation in the nuclei. Nuclear YAP/TAZ bind to TEA domain transcription factors (TEAD); promote the expression of target genes; and modulate diverse cellular functions, including proliferation, apoptosis, migration, and differentiation (Harvey et al., 2013; Hong and Guan, 2012). Consistently, loss-of-function mutations of upstream Hippo pathway components, or overexpression of YAP, lead to overgrowth and tumorigenesis in many tissues (Pan, 2010; Schlegelmilch et al., 2011; Zhou et al., 2009, 2011).

Previously, it has been shown that multiple upstream signals, such as cell-cell contact (Zhao et al., 2007), mechanical forces and cytoskeletal reorganization (Dupont et al., 2011; Zhao et al., 2012), and serum lipids and their receptors (Miller et al., 2012; Yu et al., 2012), could modulate YAP localization and S127 phosphorylation through Hippo-pathway-kinases-dependent or independent mechanisms. To identify modulators of the Hippo-YAP pathway, we developed a high-content imaging assay using human embryonic kidney 293A (HEK293A) cells to directly visualize the nuclear localization of endogenous YAP. YAP nuclear localization can be quantified by the Pearson's correlation coefficient with the nuclear staining, providing a sensitive and robust cellular assay to study the regulation of YAP (Figure S1A). Using such a system, we have discovered that energy stress and inhibition of glucose metabolism could inhibit YAP, providing molecular mechanisms linking cellular metabolism to tumorigenesis.

RESULTS

Energy Stress Induces YAP Cytoplasmic Retention and S127 Phosphorylation and Inhibits Its Transcriptional Activity

Previously, we and others have discovered that serum deprivation significantly induces YAP cytoplasmic retention through serum lipids (Miller et al., 2012; Yu et al., 2012). To further study whether other nutrient and energy stress signals could modulate YAP, we screened a set of small-molecule compounds known to modulate nutrient and energy-sensing pathways, including inhibitors of glucose metabolism and ATP production, phosphatidylinositol 3-kinase (PI3K)/AKT/mTOR signaling, and growth factor

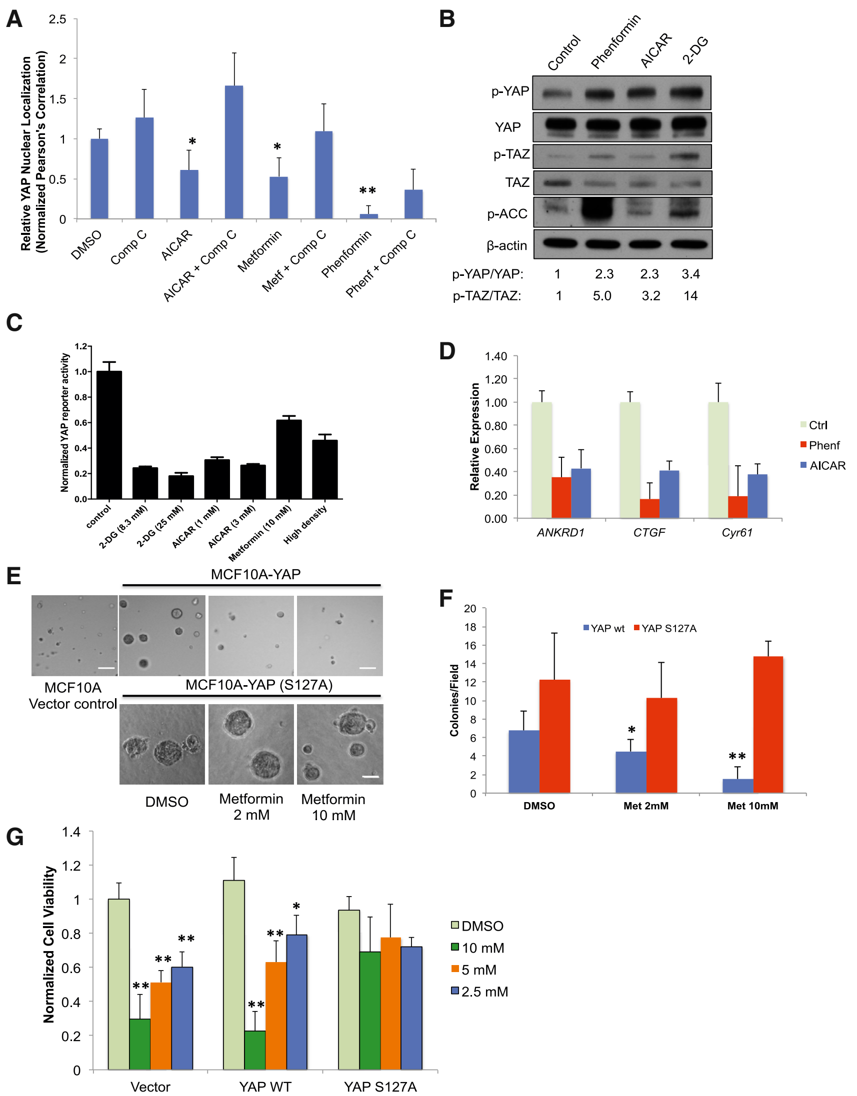

Figure 1. Energy Stress Inhibits YAP

(A) Confluent and serum-stimulated HEK293A cells were treated with DMSO control, AICAR (1 mM), metformin (10 mM), or phenformin (1 mM) with or without compound C (10 μM) for 3 hr. YAP nuclear localization is quantified by determining the Pearson's correlation coefficient of nuclear staining. Data are represented as mean, SD; n = 3. (*p < 0.03; **p < 0.001.)

(B) Small-molecule energy stressors induce YAP S127 and TAZ S89 phosphorylation in HaCaT cells. HaCaT cells were treated with DMSO (control), 1 mM phenformin, 1 mM AICAR, or 25 mM 2-DG for 6 hr.

(C) Inhibition of YAP reporter activity. HEK293 YAP reporter cells were treated with DMSO control, 2-DG (8.3 or 25 mM), AICAR (1 or 3 mM), or metformin (10 mM). Data are represented as mean, SD; n = 3.

(D) Energy stressors suppress YAP target-gene expression. HEK293A cells were treated with DMSO (ctrl), 1 mM phenformin, or 1 mM AICAR for 16 hr. Relative mRNA levels are normalized to DMSO (ctrl).

(E) MCF10A cells transduced with a vector control, YAP wild-type or YAP S127A mutant were grown on Matrigel without EGF. Cells were treated with metformin (2 mM or 10 mM) or DMSO control. The scale bar represents 100 μm.

(F) The colony numbers per field are quantified by Image J and shown in bar graph (data are represented as mean, SD; n = 4; *p < 0.05; **p < 0.0005 by comparing to the S127A mutant samples with the same treatment). WT, wild-type.

(G) Metformin dose dependently inhibits the proliferation of primary mouse hepatocellular carcinoma (HCC) cell line JF001 (*Mst1*$^{-/-}$*Mst2*$^{-/-}$). JF001 cells transduced with vector, wild-type YAP, or YAP S127A mutant were treated as indicated. Data are represented as mean, SD; n = 3; *p < 0.05; **p < 0.001 by comparing to the DMSO control.

See also Figure S1.

signaling, in the YAP translocation assay. In serum-stimulated, confluent HEK293A cells, we observed that treatment of the mitochondrial complex I inhibitor metformin (Glucophage) and its more potent analog phenformin inhibits YAP nuclear localization within 3 hr (Figures 1A and S1B). Metformin and phenformin lower cellular ATP levels, increase AMP to ATP ratio in the cell, and activate AMP-activated protein kinase (AMPK), a central cellular metabolic sensor (Hardie, 2007; Mihaylova and Shaw, 2011). Consistently, we also found that treatment with 5-aminoimidazole-4-carboxamide-1-β-riboside (AICAR), a precursor of ZMP that acts as an AMP mimetic and direct activator of AMPK (Shackelford and Shaw, 2009), has similar effects on YAP cytoplasmic retention. AICAR also potently inhibits YAP nuclear localization in cells cultured at low density (Figure S1C). In HaCaT keratinocyte cells, treatment of phenformin (1 mM) and AICAR (1 mM) for 6 hr also elevates phosphorylated YAP (p-YAP) (S127) and p-TAZ (S89) levels (Figure 1B). Phosphorylation of a well-known AMPK substrate, acetylcoenzyme A (CoA) carboxylase (ACC) indicates the activation of AMPK. Similarly, treatment of HEK293 cells with the specific AMPK activator A-769662 induces p-YAP (S127) (Cool et al., 2006; Figure S1D). Furthermore, energy stressors inhibit YAP-dependent transcription using a TEAD-binding-element-driven luciferase reporter (MCAT-YAP-Luc) and the expression of direct YAP target genes (*ANKRD1*, *CTGF*, and *CYR61*) by quantitative RT-PCR (qRT-PCR) (Figures 1C and 1D).

In addition, deprivation of glucose from the culture media and inhibition of glucose metabolism by 2-deoxy-D-glucose (2-DG) elevated p-YAP (S127) and inhibited YAP-dependent reporter activity (Figures 1B and 1C). Consistently, glucose deprivation inhibits and adding back glucose largely rescued YAP reporter activity (Figures S1E and S1F). Taken together, these data indicate that energy stress and direct activation of AMPK could inhibit YAP. Similar effects were observed in other cell types, although less significantly in fibroblast cells such as NIH 3T3 (Figure S1G). These effects are independent from inhibition of cell growth, as other antiproliferative compounds, including inhibitors of PI3K, AKT, mTOR, and CDK4 (wortmannin, LY294002, rapamycin, and roscovitine), have little effect on p-YAP induction under similar conditions (Figures S1H and S1I). Taken together, these results suggest that inhibition of YAP activity by energy stress could be a conserved and direct signaling event.

Energy Stress Inhibits YAP-Dependent Transformation and Cancer Cell Proliferation

Expression of YAP in MCF10A cells disrupts the normal acinar structures and promotes epidermal growth factor (EGF)-independent growth in Matrigel (Overholtzer et al., 2006; Zhang et al., 2009). To evaluate whether energy stress could inhibit YAP oncogenic activity, we tested metformin in MCF10A cells transduced with YAP, constitutively active YAP S127A mutant, and a vector control. Treatment with metformin (2 mM and 10 mM) showed a significant and dose-dependent reduction in colony number in cells expressing wild-type YAP (Figures 1E and 1F). Although the mean colony size is decreased upon metformin treatment, this effect was not statistically significant due to high variation of the size measurement in 3D culture (Figure S1J). The significant colony number inhibition likely reflects the inhibition of YAP-mediated cell survival rather than cell growth. In contrast, metformin did not inhibit colony formation in cells expressing YAP S127A mutant, suggesting that the effects of metformin are specifically through the inhibition of YAP nuclear localization. Consistently, the expression of YAP target genes (*CTGF* and *CYR61*) is inhibited by metformin in wild-type YAP-expressing cells, whereas expression of YAP S127A confers resistance (Figure S1K).

Mice lacking Mst1/Mst2 in the liver develop aggressive YAP-dependent hepatocellular carcinoma (HCC). We tested whether energy stress would block the proliferation of HCC cells isolated from liver-specific *Mst1*$^{-/-}$*Mst2*$^{-/-}$ mice (Zhou et al., 2009). Mouse work was done with Institutional Animal Care and Use Committee approval at Massachusetts General Hospital and in strict accord with good animal practice as defined by the Office of Laboratory Animal Welfare. Indeed, metformin dose dependently inhibits the proliferation of an HCC cell line (JF001). Expression of YAP S127A mutant confers resistance to the compound treatment, confirming that metformin inhibits HCC proliferation through the inhibition of YAP (Figure 1G). Taken together, our results illustrate that energy stress can block YAP-dependent transformation and cancer cell proliferation.

Energy Stress Inhibits YAP Involving AMPK, Lats1/Lats2 Kinases, and the Tight-Junction Protein AMOTL1

To further explore the mechanisms, we treated wild-type and AMPK-null (AMPK$\alpha1^{-/-}\alpha2^{-/-}$) mouse embryonic fibroblasts (MEFs) with 2-DG (25 mM) or phenformin (1 mM) for 12 hr. 2-DG and phenformin increased p-ACC, as well as p-YAP (S127) in wild-type MEFs, albeit to a lesser extent than in epithelial cells. In AMPK-null MEFs, p-YAP induced by phenformin and 2-DG was largely inhibited, suggesting that AMPK activity is necessary for p-YAP induction (Figure 2A). AMPK-null MEFs also have lower basal p-YAP levels compared to wild-type MEFs, suggesting that loss of AMPK might lead to YAP activation. Moreover, we found that a small-molecule AMPK inhibitor, compound C, blocks AICAR, metformin, and phenformin-induced YAP cytoplasmic retention (Figures 1A, S1B, and S1C). Because compound C might also inhibit other protein kinases (Bain et al., 2007), we used small interfering RNAs (siRNAs) targeting AMPKα1 and AMPKα2 to confirm the effects. The siRNAs (~90% knockdown efficiency) decreased p-ACC and greatly inhibited p-YAP induced by phenformin, suggesting that AMPK is indeed required to mediate the regulation of YAP (Figure 2B). Consistently, we also observed that siRNAs targeting AMPKα1 and AMPKα2 rescued the effects of metformin and phenformin on YAP nuclear localization (Figures 2C and S2A). Altogether, these data show that the cellular energy sensor AMPK is required to mediate YAP regulation in response to metabolic and energy stress.

To probe whether AMPK-mediated YAP inhibition requires upstream core Hippo pathway kinases, we first tested the effects in *Mst1*$^{-/-}$*Mst2*$^{-/-}$ HCCs. Interestingly, metformin treatment induces and cotreatment of compound C inhibits p-YAP (S127) in these cells, suggesting that Mst1/Mst2 kinases are dispensable to inhibit YAP (Figure 2D). This is also consistent with our data that metformin blocks the proliferation of *Mst1*$^{-/-}$*Mst2*$^{-/-}$ HCCs (Figure 1H). We then used siRNAs to silence Lats1 and Lats2 (~90% knockdown; Figure S2B), which decreased the basal level of p-YAP and completely blocked the effects of energy stressors (Figure 2E), suggesting that energy-stress-mediated YAP phosphorylation requires Lats1/Lats2 kinases.

Next, we examined the changes of known Hippo pathway regulators upon energy stress. We found that phenformin treatment significantly increased the protein levels of angiomotin-like 1 (AMOTL1) by 7.3-fold. The protein levels of other motin family proteins (AMOT and AMOTL2) also increased, although less significantly (Figure 3A). In total, the levels of motin proteins increased more than 12-fold upon phenformin treatment. AMOT, AMOTL1, and AMOTL2 are tight junction proteins that inhibit YAP through three mechanisms: (1) binding to and sequestering YAP out of nuclei (Yi et al., 2011; Zhao et al., 2011); (2) binding to and enhancing Lats1/Lats2 activation (Paramasivam et al., 2011); and (3) reducing the stability of YAP by promoting its ubiquitination (Adler et al., 2013a). This is consistent with our observation that, upon metabolic stress, changes in YAP translocation are more quickly detected than its S127 phosphorylation, suggesting that direct sequestration and enhanced Lats1/Lats2 activity both play roles in the regulation. Indeed, we observed moderate activation of Lats1 (p-Lats1 S909) by 2.2-fold with phenformin treatment. Other upstream Hippo pathway components, such as NF2 and MST2, were not significantly changed. We then evaluated the mRNA levels of motin family members by qRT-PCR. We observed that phenformin treatment did not significantly increase the mRNA levels of AMOTL1 and AMOTL2 and AMOT mRNA levels increase by ~2-fold (Figure S3A). We chose to focus our studies on AMOTL1 in energy-stress-mediated YAP inhibition, as its changes are the most significant.

To test whether metabolic stress could stabilize AMOTL1, we treated cells with metformin or DMSO control, together the with protein synthesis inhibitor cycloheximide, and analyzed the protein levels of endogenous AMOTL1 by western blotting at different time points (Figure 3B). We observed that the half-life of endogenous AMOTL1 increases from 15.4 to 56.2 min with metformin treatment (Figure 3C). Therefore, energy stress might

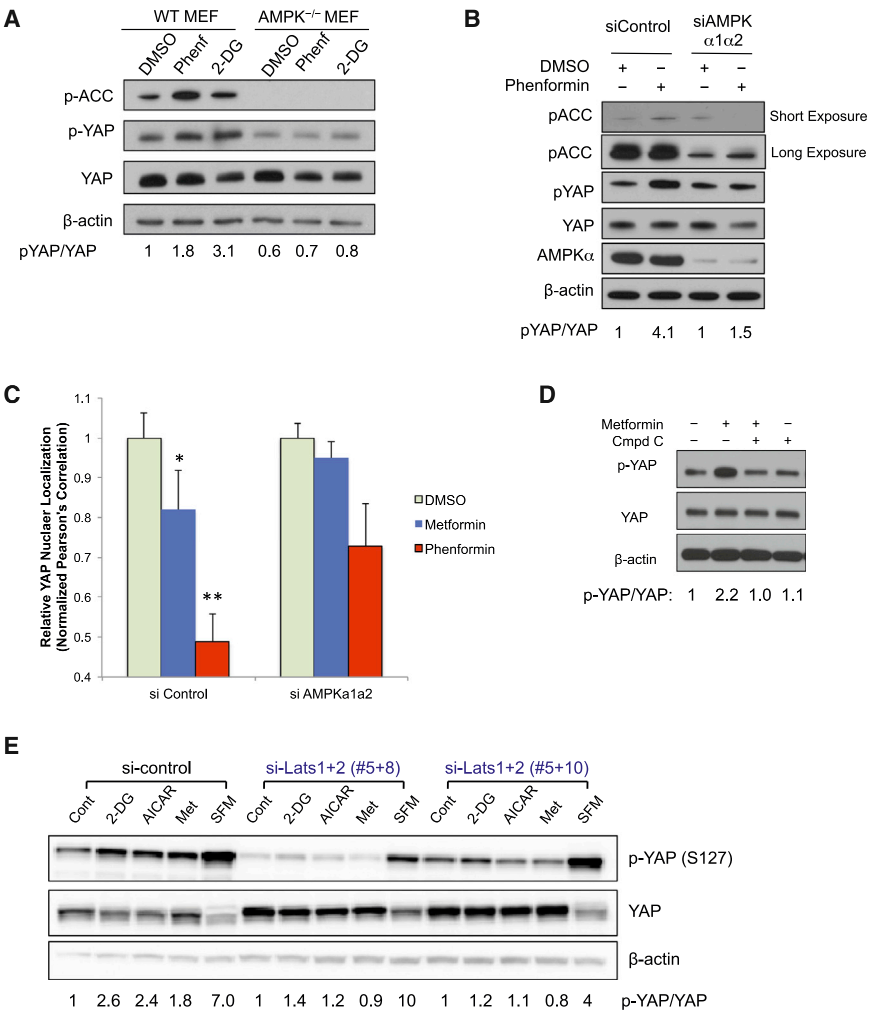

Figure 2. Energy Stress Inhibits YAP through AMPK and Lats1/Lats2

(A) AMPK is required for YAP inhibition. Wild-type or AMPK$^{-/-}$ (AMPKα1α2 double knockout) MEFs were treated with DMSO control, 2-DG (25 mM), or phenformin (1 mM) for 12 hr. Cells were then harvested for western blot analysis.

(B) HaCaT cells were transfected with siRNAs targeting AMPKα1 and AMPKα2 and then treated for 16 hr with DMSO or phenformin (1 mM).

(C) siRNAs targeting AMPKα1 and AMPKα2 blocks YAP cytoplasmic retention. Cells were transfected with siRNAs targeting AMPK and then treated for 16 hr with DMSO, metformin (10 mM), or phenformin (1 mM). YAP nuclear localization is quantified by determining the Pearson's correlation coefficient between YAP-positive areas with the nuclear staining. Data are represented as mean, SD; n = 3. *$p < 0.05$; **$p < 0.001$ by comparing to the DMSO control.

(D) HCCs were isolated from tumors derived from liver-specific *Mst1*$^{-/-}$*Mst2*$^{-/-}$ mice. Cells are treated with metformin (10 mM) or cotreated with compound C (10 μM) for 8 hr. p-YAP levels were evaluated by western blot.

(E) HEK293A cells were transfected with siRNA control or siRNA targeting Lats1 and Lats2 (no. 5+8 or no. 5+10). Cells were treated with AICAR (1 mM) or metformin (10 mM) for 8 hr, serum-free media (SFM) (3 hr), or 2-DG (25 mM; 3 hr). Cells were then harvested for western blot analysis of p-YAP (S127).

See also Figure S2.

stabilize the AMOTL1 protein and thus increase its steady-state protein levels, leading to YAP inhibition.

To confirm that motin proteins are required to mediate the effects, we transfected siRNAs targeting AMOT and AMOTL1 with GFP into HEK293A cells and treated the cells with 1 mM phenformin or DMSO. The siRNAs effectively knock down AMOT and AMOTL1 (Figure S3B). In siRNA-transfected cells (GFP+), we observed that knocking down AMOT/AMOTL1 blocked phenformin effects. In the nontransfected cells (GFP−), phenformin remains effective, serving as a good internal control (Figures 3D and S3C). In HaCaT cells, AMOTL1 small hairpin RNA (shRNA) alone could sufficiently block phenformin-induced p-YAP (Figure 3E). In addition, when AMOTL1 is silenced by shRNA, inhibition of YAP target genes expression (*CTGF*, *Cyr61*, and *ANKD1*) by phenformin could be significantly rescued (Figure S3D). Most importantly, the growth inhibition of these cells by phenformin and metformin could also be significantly rescued when AMOTL1 is silenced (Figure 3F). Taken together, these results suggest that the motin family proteins, particularly AMOTL1, are involved in the regulation of YAP in response to energy stress.

AMPK Directly Phosphorylates AMOTL1 at S793

We then set out to study how AMPK regulates AMOTL1. To test whether motin proteins could be direct substrates of AMPK, we carried out a bioinformatics search for conserved AMPK substrate motifs (Dale et al., 1995; Gwinn et al., 2008; Scott et al., 2002). We found that all motin proteins contain AMPK substrate motifs (AMOTL1 S793, AMOT S787, and AMOTL2 S667), all of which are evolutionarily conserved among vertebrates (Figure 4A). We then performed coimmunoprecipitation experiments and found that the AMPKα subunit directly binds to AMOTL1 (Figure S4A). To confirm that AMOTL1 could be phosphorylated upon AMPK activation in cells, we carried out phosphoproteomic studies using FLAG-AMOTL1 isolated from cells treated with DMSO control, metformin, or cotreated with metformin and compound C. We detected nonphosphorylated peptides (peak A), peptides phosphorylated at an adjacent site S805 (peak B), peptides phosphorylated at the predicted AMPK site S793 (peak C), and peptides with double phosphorylation at S793 and S805 (peak D; Figure 4B) by liquid chromatography-tandem mass spectrometry (LC-MS/MS) methods (Figure S4B). We then quantified their relative abundance by calculating the area under the curve (AUC). Treatment with metformin increased the abundance of peptide fragments containing p-S793 (peaks C and D), and cotreatment with compound

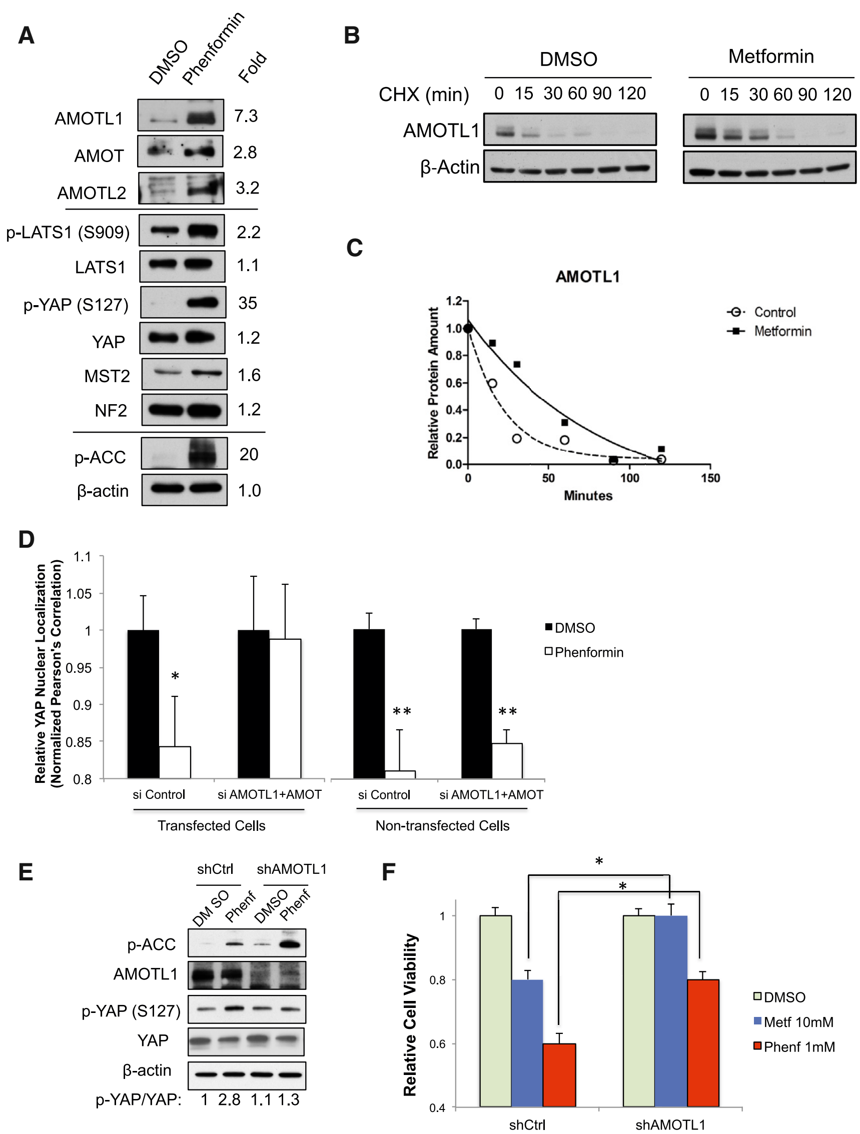

Figure 3. Endogenous AMOTL1 Is Stabilized in Response to Energy Stress and Required to Mediate AMPK-Induced YAP-Cytoplasmic Retention and S127 Phosphorylation

(A) HEK293A cells were treated with DMSO control or phenformin (1 mM) for 16 hr. Protein levels of Hippo pathway components (AMOTL1, AMOT, AMOTL2, p-YAP, YAP, p-Lats1, Lats1, MST2, and NF2) were analyzed by western blots.

(B) Cells were treated with metformin (10 mM) for 4 hr and with cycloheximide (CHX) with indicated time. Protein levels of endogenous AMOTL1 were analyzed by western blots.

(C) Protein levels from (B) were quantified by densitometry of the bands. Projected degradation curve of AMOTL1 was plotted and fitted using Prism software.

(D) HEK293A cells were transfected with siRNAs targeting AMOT and AMOTL1, with GFP to mark transfected cells. Cells were treated with phenformin (1 mM) or DMSO. YAP nuclear localization is quantified by determining the Pearson's correlation coefficient in GFP-positive (transfected) or GFP-negative (nontransfected) cells. Data are represented as mean, SD; n = 3. *p < 0.02; **p < 0.001 by comparing to the DMSO controls.

(E) HaCaT cells were transfected with shRNA targeting AMOTL1. Cells were treated with DMSO control or phenformin (1 mM), and p-YAP level is analyzed.

(F) Cells were transfected shRNA targeting AMOTL1 and then treated with DMSO, metformin (10 mM), or phenformin (1 mM) for 48 hr. The cell proliferation is determined by measuring the cell viability. Data are represented as mean, SD; n = 3 (*p < 0.01).

See also Figure S3.

C dramatically decreased p-S793 peptides abundance, suggesting that activation of AMPK leads to increased phosphorylation of AMOTL1 at S793 in cells (Figure 4C). In addition, the phosphorylation levels of the adjacent S805 site are independent of AMPK activation and inhibition, serving as an ideal internal control (Figure 4B).

To confirm that S793 is directly phosphorylated by AMPK, we generated an AMOTL1 (S793A) mutant construct. Indeed, purified AMPK kinase could phosphorylate AMOTL1 wild-type, but not the S793A mutant in vitro (Figure 4D). In addition, we quantified the radioactivity of the phosphorylated AMOTL1 in this assay. We observed the phosphorylation stoichiometry of 0.78 mol of phosphate incorporation per mole of AMOTL1 (78% phosphorylated). These results suggest that S793 is indeed an AMPK substrate site. Furthermore, we utilized a Phos-tag gel to visualize phosphorylated and nonphosphorylated species of AMOTL1. In DMSO-treated cells, 12% of the AMOTL1 protein is phosphorylated. Upon treatment with A-769662 or phenformin, the percentage of phosphorylated AMOTL1 increases to 37% and 73%, respectively (Figure 4E). Thus, AMPK activation increases the amount of phosphorylated AMOTL1 in cells. Next, we generated a phosphospecific antibody against p-S793 of AMOTL1. Although the antibody is too weak to reliably detect endogenous AMOTL1 phosphorylation, it showed good specificity and sensitivity toward exogenous wild-type, but not S793 mutants (Figure S4C). We transfected HaCaT cells with FLAG-AMOTL1 and treated the cells with phenformin or DMSO control for 1 or 2 hr. We observed that the AMOTL1 p-S793 increased within 1 hr (Figure 4F), suggesting that its phosphorylation is indeed enhanced by AMPK activation. We also observed that exogenous FLAG-AMOTL1 has high basal S793 phosphorylation levels, possibly resulting from the basal AMPK activity in the cells (Figures 4F and 4G). Consistently, when AMPKα1/AMPKα2 subunits are silenced by siRNAs (with knockdown efficiency of ~50%) in HEK293A cells, we observed a significant decrease in the basal p-AMOTL1 levels (Figure 4G), thus suggesting that inhibition of AMPK could inhibit p-AMOTL1. With

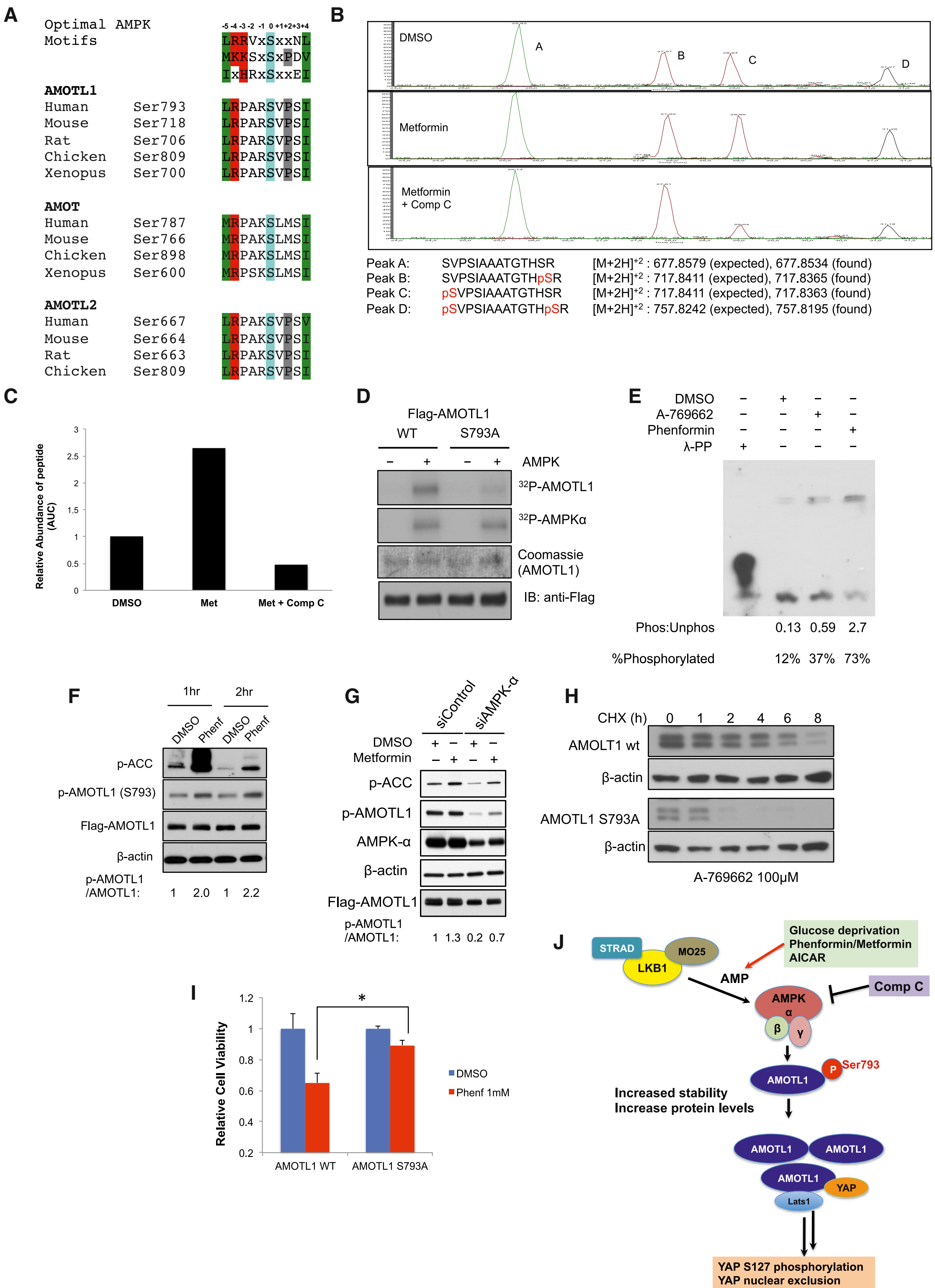

Figure 4. AMPK Directly Phosphorylates AMOTL1 S793, Leading to Its Stabilization and YAP Inhibition

(A) Alignment of the conserved AMPK substrate motifs in angiomotin family proteins (AMOTL1, AMOT, and AMOTL2) of different species.

(B) LC-MS/MS studies of phosphorylation of AMOTL1 S793. FLAG-AMOTL1 was purified from HEK293A cells treated with metformin (10 mM) or metformin and compound C (10 μM). Extracted ion chromatographs of peptides containing S793 were shown. Peak A, unphosphorylated peptide; peak B, peptide with p-S805; peak C, peptide with p-S793; peak D, peptide with p-S793 and p-S805.

(legend continued on next page)

the decrease of basal p-AMOTL1 levels, the fold induction of p-AMOTL1 by metformin treatment is more significant, suggesting that the phosphorylation of exogenous AMOTL1 at S793 indeed could be regulated by AMPK (Figure 4G). Collectively, these data suggest that AMOTL1 is indeed an AMPK substrate and AMOTL1 S793 could be phosphorylated by AMPK directly.

AMPK-Mediated AMOTL1 S793 Phosphorylation Leads to Increased Protein Stability

We then probed the functional consequences of AMOTL1 S793 phosphorylation. We transfected HEK293T cells with either wild-type or S793A AMOTL1 and treated cells with AMPK activator A-769662 (100 μM). We then measured the protein half-life of wild-type and AMOTL1 S793A by cycloheximide chase followed by western blotting (Figure 4H). We found that the half-life of the S793A mutant is markedly shorter than the wild-type, suggesting that loss of S793 phosphorylation destabilizes AMOTL1. Furthermore, dephosphorylation of AMOTL1 by compound C treatment also dramatically decreased the half-life of endogenous AMOTL1 (Figure S4D). Because Lats1/Lats2 phosphorylation of AMOT at S175 has been implicated in regulation of its localization and stability (Adler et al., 2013b; Dai et al., 2013), we tested whether Lats1/Lats2 are required to stabilize AMOTL1 upon energy stress. We found that, although knocking down Lats1/Lats2 decreased basal AMOTL1 protein levels, it had no effect on the AMPK-activator-mediated increase of AMOTL1 protein levels (Figure S4E). Further studies are needed to elucidate the cooperation between the Lats1/Lats2 and AMPK phosphorylation sites on motin proteins.

To test whether AMOTL1 S793 phosphorylation is functionally involved in YAP inhibition, we knocked down endogenous AMOTL1 using shRNA and then overexpress the shRNA-resistant version of AMOTL1 wild-type or AMOTL1 S793A mutant. Interestingly, we found that, in cells expressing wild-type AMOTL1, phenformin could significantly inhibit YAP target gene expression. However, in cells expressing AMOTL1 S793A mutant, phenformin failed to inhibit YAP target genes (Figure S4F). Furthermore, in cells expressing wild-type AMOTL1, phenformin could potently inhibit cell proliferation, whereas expressing AMOTL1 S793A mutant significantly rescues the inhibitory effects of phenformin (Figure 4I). These results suggest that AMOTL1 S793 phosphorylation could modulate YAP functions in response to energy stress and could be one of the mechanisms leading to YAP inhibition.

DISCUSSION

Here, we propose a signaling mechanism (Figure 4J), in which cellular energy level is an upstream regulator of Hippo signaling. We found that energy stress activates AMPK, stabilizes AMOTL1, and leads to YAP inhibition. Although glucose deprivation and metformin treatment could activate AMPK relatively quickly (in 1 hr; Nguyen et al., 2013), sustained AMPK activation (~2–6 hr) was required to inhibit YAP. This is consistent with our proposed mechanism in which phosphorylation of AMOTL1 by AMPK leads to AMOTL1 protein accumulation due to its increased half-life. However, other possible AMPK substrates (Kibra, ZO-2, and YAP) and other motin family members could also be involved in the regulation of YAP. Therefore, further studies to characterize them as AMPK substrates would shed insights into the mechanisms of YAP regulation. In addition, it is also possible that other AMPK-related kinases (such as SIK or microtubule affinity-regulating kinase [MARK]) could mediate the basal phosphorylation of AMOTL1 and AMPK activation boosts the existing phosphorylation in response to metabolic stress, which is not uncommon in AMPK-regulated substrates (Shackelford and Shaw, 2009).

Among the motin family proteins, AMOTL1 might be the major mediator of the effects. We could not detect phosphorylation of the predicted AMPK motif (S787) in AMOT by mass spectrometry. Other non-AMPK sites (S97 and S714) are phosphorylated upon metformin treatment in mass spectrometry studies (Figure S4G). These results suggest that other kinases downstream of AMPK or less-stringent AMPK substrate sites might be involved. Therefore, AMOT might be regulated differently than AMOTL1, and future studies are needed to elucidate the regulation of AMOT and AMOTL2 in response to energy stress and their roles in YAP regulation.

LKB1/STK11 is a known tumor suppressor (Shackelford and Shaw, 2009) and a major upstream regulator of AMPK. Our results suggest that loss of LKB1 and AMPK activities might contribute to tumorigenesis through destabilizing AMOTL1, leading to hyperactivation of YAP. A recent study has shown that LKB1 acts through the MARK family to regulate the localization of Scribble (Mohseni et al., 2014). Our results and the results of Mohseni et al. (2014) suggest that there are multiple pathways downstream of LKB1 to regulate YAP activity. This could have important implications for the treatment of LKB1-dependent tumors. Recent work by the Cancer Genome Atlas Project has

(C) The abundance of the peptides was quantified by measuring the area under the curve (AUC) in the spectra.
(D) Recombinant AMPK phosphorylates AMOTL1 wild-type, but not S793A mutant, in vitro. IB, immunoblot.
(E) HEK239T cells were treated for 8 hr with DMSO (control), 1 μM A-769662, or 1 mM phenformin. Protein lysates were then analyzed by Phos-Tag SDS-PAGE followed by western blotting with anti-AMOTL1.
(F) Phenformin treatment increased AMOTL1 S793 phosphorylation. An antibody recognizing p-AMOTL1 (S793) was used in western blot. HaCaT cells were transfected with FLAG-AMOTL1 and then treated with DMSO or phenformin (1 mM) for 1 or 2 hr.
(G) Knockdown of AMPK decreased the levels of p-AMOTL1. Cells were transfected with siRNAs targeting AMPKα1 and AMPKα2 and FLAG-AMOTL1. Cells were then treated with metformin (10 mM) or DMSO control. p-AMOTL1 levels were determined by using a phosphospecific antibody recognizing AMOTL1 S793.
(H) AMOTL1 S793A has a shorter half-life than wild-type AMOTL1. HEK293T cells transfected with either wild-type or S793A mutant AMOTL1 were treated for 16 hr with A-769662 and then treated for the indicated time with cycloheximide (CHX).
(I) Cells were transfected with AMOTL1 wild-type or S793A mutant and then treated with DMSO control or phenformin (1 mM) for 48 hr. The cell viability is determined by CellTiter Glo. Data are represented as mean, SD; n = 3 (*$p < 0.01$).
(J) A proposed model of energy-stress-mediated YAP inhibition.
See also Figure S4.

identified mutations of AMOTL1 at the AMPK recognition motif (R789C, P790I, and R792H) in multiple cancers. Although at low frequencies, such mutations might lead to loss of AMPK-mediated S793 phosphorylation and promote YAP activation in these cancers. In summary, our studies have shown that cellular energy sensor AMPK could regulate YAP by directly phosphorylating and stabilizing tight-junction protein AMOTL1, connecting energy sensing to the regulation of Hippo pathway.

EXPERIMENTAL PROCEDURES

Immunofluorescence Staining, YAP Translocation Assay, and Imaging Analysis

Cells were fixed and then stained with primary antibody (anti-YAP). The images were acquired by high-throughput confocal microscopy (Opera High Content Screening System). Four images/well were captured using a 20× objective at a resolution of ~0.65 μm/pixels. The images of YAP immunostaining and nuclear Hoechst were analyzed with a custom Acapella (PerkinElmer) script as previously reported or with CellProfiler (Carpenter et al., 2006). YAP nuclear/cytoplasmic translocation was defined using the Pearson's correlation coefficient (R) between the YAP and the Hoechst fluorescence channels across each pixel of the cellular object detected.

SUPPLEMENTAL INFORMATION

Supplemental Information includes Supplemental Discussion, Supplemental Experimental Procedures, and four figures and can be found with this article online at http://dx.doi.org/10.1016/j.celrep.2014.09.036.

AUTHOR CONTRIBUTIONS

J.Y., M.D., J.L., and X.W. conceived the concepts and designed the experiments. E.C.P. and J.M.A. performed mass spec studies of AMOTL1 and AMOT, respectively. J.Y., M.D., P.C., M.H., S.Z., J.F., N.B., C.-H. S., and B.Z. performed the cell biology and biochemistry experiments. All authors analyzed the data, and J.Y., M.D., and X.W. wrote the manuscript.

ACKNOWLEDGMENTS

This work is supported by MGH, HSCI Seed Grant, Children's Tumor Foundation, American Cancer Society (124929-RSG-13-291-01-TBE), NIH/NCI R01CA181537 (X.W.), and NIH/NCI R01CA166717 (B.Z.). We thank Drs. K.-L. Guan, A. Schmitt, J. Brugge, M. Sudol, D. McCollum, J. Avruch, K. Laderoute, and L. Cantley for constructs, antibodies, cell lines, or discussions. E.C.P., M.H., and J.L. are employees of Novartis.

Received: December 15, 2013
Revised: August 18, 2014
Accepted: September 18, 2014
Published: October 16, 2014

REFERENCES

Adler, J.J., Heller, B.L., Bringman, L.R., Ranahan, W.P., Cocklin, R.R., Goebl, M.G., Oh, M., Lim, H.S., Ingham, R.J., and Wells, C.D. (2013a). Amot130 adapts atrophin-1 interacting protein 4 to inhibit yes-associated protein signaling and cell growth. J. Biol. Chem. *288*, 15181–15193.

Adler, J.J., Johnson, D.E., Heller, B.L., Bringman, L.R., Ranahan, W.P., Conwell, M.D., Sun, Y., Hudmon, A., and Wells, C.D. (2013b). Serum deprivation inhibits the transcriptional co-activator YAP and cell growth via phosphorylation of the 130-kDa isoform of Angiomotin by the LATS1/2 protein kinases. Proc. Natl. Acad. Sci. USA *110*, 17368–17373.

Bain, J., Plater, L., Elliott, M., Shpiro, N., Hastie, C.J., McLauchlan, H., Klevernic, I., Arthur, J.S., Alessi, D.R., and Cohen, P. (2007). The selectivity of protein kinase inhibitors: a further update. Biochem. J. *408*, 297–315.

Carpenter, A.E., Jones, T.R., Lamprecht, M.R., Clarke, C., Kang, I.H., Friman, O., Guertin, D.A., Chang, J.H., Lindquist, R.A., Moffat, J., et al. (2006). CellProfiler: image analysis software for identifying and quantifying cell phenotypes. Genome Biol. *7*, R100.

Cool, B., Zinker, B., Chiou, W., Kifle, L., Cao, N., Perham, M., Dickinson, R., Adler, A., Gagne, G., Iyengar, R., et al. (2006). Identification and characterization of a small molecule AMPK activator that treats key components of type 2 diabetes and the metabolic syndrome. Cell Metab. *3*, 403–416.

Dai, X., She, P., Chi, F., Feng, Y., Liu, H., Jin, D., Zhao, Y., Guo, X., Jiang, D., Guan, K.L., et al. (2013). Phosphorylation of angiomotin by Lats1/2 kinases inhibits F-actin binding, cell migration, and angiogenesis. J. Biol. Chem. *288*, 34041–34051.

Dale, S., Wilson, W.A., Edelman, A.M., and Hardie, D.G. (1995). Similar substrate recognition motifs for mammalian AMP-activated protein kinase, higher plant HMG-CoA reductase kinase-A, yeast SNF1, and mammalian calmodulin-dependent protein kinase I. FEBS Lett. *361*, 191–195.

Dong, J., Feldmann, G., Huang, J., Wu, S., Zhang, N., Comerford, S.A., Gayyed, M.F., Anders, R.A., Maitra, A., and Pan, D. (2007). Elucidation of a universal size-control mechanism in Drosophila and mammals. Cell *130*, 1120–1133.

Dupont, S., Morsut, L., Aragona, M., Enzo, E., Giulitti, S., Cordenonsi, M., Zanconato, F., Le Digabel, J., Forcato, M., Bicciato, S., et al. (2011). Role of YAP/TAZ in mechanotransduction. Nature *474*, 179–183.

Gwinn, D.M., Shackelford, D.B., Egan, D.F., Mihaylova, M.M., Mery, A., Vasquez, D.S., Turk, B.E., and Shaw, R.J. (2008). AMPK phosphorylation of raptor mediates a metabolic checkpoint. Mol. Cell *30*, 214–226.

Hardie, D.G. (2007). AMP-activated/SNF1 protein kinases: conserved guardians of cellular energy. Nat. Rev. Mol. Cell Biol. *8*, 774–785.

Harvey, K., and Tapon, N. (2007). The Salvador-Warts-Hippo pathway - an emerging tumour-suppressor network. Nat. Rev. Cancer *7*, 182–191.

Harvey, K.F., Pfleger, C.M., and Hariharan, I.K. (2003). The Drosophila Mst ortholog, hippo, restricts growth and cell proliferation and promotes apoptosis. Cell *114*, 457–467.

Harvey, K.F., Zhang, X., and Thomas, D.M. (2013). The Hippo pathway and human cancer. Nat. Rev. Cancer *13*, 246–257.

Hong, W., and Guan, K.L. (2012). The YAP and TAZ transcription co-activators: key downstream effectors of the mammalian Hippo pathway. Semin. Cell Dev. Biol. *23*, 785–793.

Mihaylova, M.M., and Shaw, R.J. (2011). The AMPK signalling pathway coordinates cell growth, autophagy and metabolism. Nat. Cell Biol. *13*, 1016–1023.

Miller, E., Yang, J., DeRan, M., Wu, C., Su, A.I., Bonamy, G.M., Liu, J., Peters, E.C., and Wu, X. (2012). Identification of serum-derived sphingosine-1-phosphate as a small molecule regulator of YAP. Chem. Biol. *19*, 955–962.

Mohseni, M., Sun, J., Lau, A., Curtis, S., Goldsmith, J., Fox, V.L., Wei, C., Frazier, M., Samson, O., Wong, K.K., et al. (2014). A genetic screen identifies an LKB1-MARK signalling axis controlling the Hippo-YAP pathway. Nat. Cell Biol. *16*, 108–117.

Nguyen, H.B., Babcock, J.T., Wells, C.D., and Quilliam, L.A. (2013). LKB1 tumor suppressor regulates AMP kinase/mTOR-independent cell growth and proliferation via the phosphorylation of Yap. Oncogene *32*, 4100–4109.

Overholtzer, M., Zhang, J., Smolen, G.A., Muir, B., Li, W., Sgroi, D.C., Deng, C.X., Brugge, J.S., and Haber, D.A. (2006). Transforming properties of YAP, a candidate oncogene on the chromosome 11q22 amplicon. Proc. Natl. Acad. Sci. USA *103*, 12405–12410.

Pan, D. (2007). Hippo signaling in organ size control. Genes Dev. *21*, 886–897.

Pan, D. (2010). The hippo signaling pathway in development and cancer. Dev. Cell *19*, 491–505.

Paramasivam, M., Sarkeshik, A., Yates, J.R., 3rd, Fernandes, M.J., and McCollum, D. (2011). Angiomotin family proteins are novel activators of the LATS2 kinase tumor suppressor. Mol. Biol. Cell *22*, 3725–3733.

Schlegelmilch, K., Mohseni, M., Kirak, O., Pruszak, J., Rodriguez, J.R., Zhou, D., Kreger, B.T., Vasioukhin, V., Avruch, J., Brummelkamp, T.R., and

Camargo, F.D. (2011). Yap1 acts downstream of α-catenin to control epidermal proliferation. Cell *144*, 782–795.

Scott, J.W., Norman, D.G., Hawley, S.A., Kontogiannis, L., and Hardie, D.G. (2002). Protein kinase substrate recognition studied using the recombinant catalytic domain of AMP-activated protein kinase and a model substrate. J. Mol. Biol. *317*, 309–323.

Shackelford, D.B., and Shaw, R.J. (2009). The LKB1-AMPK pathway: metabolism and growth control in tumour suppression. Nat. Rev. Cancer *9*, 563–575.

Udan, R.S., Kango-Singh, M., Nolo, R., Tao, C., and Halder, G. (2003). Hippo promotes proliferation arrest and apoptosis in the Salvador/Warts pathway. Nat. Cell Biol. *5*, 914–920.

Wu, S., Huang, J., Dong, J., and Pan, D. (2003). hippo encodes a Ste-20 family protein kinase that restricts cell proliferation and promotes apoptosis in conjunction with salvador and warts. Cell *114*, 445–456.

Yi, C., Troutman, S., Fera, D., Stemmer-Rachamimov, A., Avila, J.L., Christian, N., Persson, N.L., Shimono, A., Speicher, D.W., Marmorstein, R., et al. (2011). A tight junction-associated Merlin-angiomotin complex mediates Merlin's regulation of mitogenic signaling and tumor suppressive functions. Cancer Cell *19*, 527–540.

Yu, F.X., Zhao, B., Panupinthu, N., Jewell, J.L., Lian, I., Wang, L.H., Zhao, J., Yuan, H., Tumaneng, K., Li, H., et al. (2012). Regulation of the Hippo-YAP pathway by G-protein-coupled receptor signaling. Cell *150*, 780–791.

Zhang, J., Ji, J.Y., Yu, M., Overholtzer, M., Smolen, G.A., Wang, R., Brugge, J.S., Dyson, N.J., and Haber, D.A. (2009). YAP-dependent induction of amphiregulin identifies a non-cell-autonomous component of the Hippo pathway. Nat. Cell Biol. *11*, 1444–1450.

Zhao, B., Wei, X., Li, W., Udan, R.S., Yang, Q., Kim, J., Xie, J., Ikenoue, T., Yu, J., Li, L., et al. (2007). Inactivation of YAP oncoprotein by the Hippo pathway is involved in cell contact inhibition and tissue growth control. Genes Dev. *21*, 2747–2761.

Zhao, B., Li, L., Lu, Q., Wang, L.H., Liu, C.Y., Lei, Q., and Guan, K.L. (2011). Angiomotin is a novel Hippo pathway component that inhibits YAP oncoprotein. Genes Dev. *25*, 51–63.

Zhao, B., Li, L., Wang, L., Wang, C.Y., Yu, J., and Guan, K.L. (2012). Cell detachment activates the Hippo pathway via cytoskeleton reorganization to induce anoikis. Genes Dev. *26*, 54–68.

Zhou, D., Conrad, C., Xia, F., Park, J.S., Payer, B., Yin, Y., Lauwers, G.Y., Thasler, W., Lee, J.T., Avruch, J., and Bardeesy, N. (2009). Mst1 and Mst2 maintain hepatocyte quiescence and suppress hepatocellular carcinoma development through inactivation of the Yap1 oncogene. Cancer Cell *16*, 425–438.

Zhou, D., Zhang, Y., Wu, H., Barry, E., Yin, Y., Lawrence, E., Dawson, D., Willis, J.E., Markowitz, S.D., Camargo, F.D., and Avruch, J. (2011). Mst1 and Mst2 protein kinases restrain intestinal stem cell proliferation and colonic tumorigenesis by inhibition of Yes-associated protein (Yap) overabundance. Proc. Natl. Acad. Sci. USA *108*, E1312–E1320.